

Self-diffusion measurements of polycyclic aromatic hydrocarbon alkali metal salts



Roy E. Hoffman,^a Elad Shabtai,^a Mordecai Rabinovitz,^{*a} Vivekanantan S. Iyer,^b Klaus Müllen,^b Amarjit K. Rai, Eric Bayrd^c and Lawrence T. Scott^c

^a Department of Organic Chemistry, The Hebrew University of Jerusalem, Jerusalem, Israel 91904

^b Max-Planck-Institut für Polymerforschung, Ackermannweg 10, D-55021 Mainz, Germany

^c Merkert Chemistry Center, Boston College, Chestnut Hill, MA 02167-3860, USA

The solvations of various polycyclic aromatic hydrocarbon alkali metal salts are studied using their self-diffusion rates measured by NMR spectroscopy. The moiety size is more dependent on the anion than the cation. The self-diffusion rates of the neutral compounds are found to be predictable while the salts diffuse considerably slower than the unsolvated species indicating the presence of a solvent shell. The apparent moiety size is temperature dependent for the salts in ethereal solutions indicating a solvation shell of varying size.

Introduction

Synthetic organic chemists widely use dianions and polyanions of polycyclic aromatic hydrocarbons (PAHs). The ions' properties and reactivity are therefore of great importance to the organic chemist. Detailed studies have been made of their solvation state¹⁻⁷ which affects their acidity, reactivity and spectroscopic properties. There is UV and NMR spectroscopic evidence for at least a first solvation shell including observations of equilibria between contact ions and solvent separated ions. The fact that the salts are insoluble in non-polar solvents such as cyclohexane indicates a dependence on solvation. X-Ray crystallographic studies of dilithium 9,10-dihydroanthracenediide show association of the metal to a solvent.⁸ However, the total size of the solvation shell and the question of aggregation in solution is still open to speculation.

The self-diffusion constant is one physical property that can, in principle, be used to estimate the size of each moiety in solution and shed some light on solvation and aggregation. The salts under study are highly reactive and this makes the application of traditional methods of self-diffusion measurement such as Rayleigh interferometry^{9,10} and radioactive tracer studies¹¹ impractical. Greater availability of the hardware used for generating gradient pulses in commercial NMR spectrometers has made it possible to measure self-diffusion easily and accurately by NMR spectroscopy.

Results and discussion

Self-diffusion of neutral polycyclic aromatic hydrocarbons

In principle, the self-diffusion constant can be used to measure the moiety size. Under the right conditions, the Stokes–Einstein relation [eqns. (1) and (2), where D is self-diffusion constant, k_B

$$D = \frac{k_B T}{6\pi\eta r} \quad (1)$$

$$r = \frac{k_B T}{6\pi\eta D} \quad (2)$$

is the Boltzmann constant ($1.380\ 62 \times 10^{-23}$ J K⁻¹), T is temperature, η is viscosity and r is radius] can be used directly to determine the size.

The Stokes–Einstein relation holds best when the particles

Table 1 Self-diffusion constants and molecular radii of polycyclic aromatic hydrocarbons in [²H₆]THF at 298.5 K

Compound	Molecular radius/nm	$D/10^{-9}$ m ² s ⁻¹ ^a	Stokes radius/nm ^a
Benzene	0.267 10	2.31	0.18
Naphthalene	0.305 57	1.97	0.22
Anthracene	0.336 22	1.76	0.24
Pyrene	0.345 19	1.58	0.27
9-Methylanthracene	0.348 74	1.49	0.29
Corannulene	0.361 86	1.29	0.33
Tetracene	0.362 12	1.57	0.27
9,10-Dimethyl-9,10-dihydroanthracene	0.368 13	1.32	0.32
9-Phenylanthracene	0.377 99	1.23	0.34
9,10-Diphenylanthracene	0.412 13	1.04	0.41
1,8-Dicorannulenyl-octane	0.502 53	0.76	0.56
Penta- <i>tert</i> -butylcorannulene	0.513 51	0.86	0.49
Hexakis(<i>tert</i> -butylbenzo)-coronene	0.584 88	0.60	0.70

^a Self-diffusion measurements were made by the PFG-SSE NMR method and are accurate to $\pm 2\%$. The Stokes radius was calculated from the measured self-diffusion constant.

are spherical and much larger than the solvent molecules. When the particles are smaller than about five times the radius of the solvent molecules, the self-diffusion constant is significantly less than would be indicated by the Stokes–Einstein relation.¹² For non-spherical particles and especially flexible ones, there is no simple relationship with the self-diffusion constant. The polycyclic aromatic hydrocarbons that we have studied have an average radius [$r = \sqrt[3]{(3V/4\pi)}$ where V is the van der Waals volume¹²] between 0.3 and 0.6 nm. Larger polycyclic aromatic hydrocarbons are generally very insoluble so were not studied. Simple ethereal solvents have an average radius between 0.24 and 0.28 nm. Therefore, the Stokes–Einstein relation does not hold well because of the small size of polycyclic aromatic hydrocarbon molecules relative to the solvent molecules. Most polycyclic aromatic hydrocarbons are planar but all are decidedly not spherical. Some, such as 9,10-diphenylanthracene and 1,8-dicorannulenyl-octane, are flexible. The self-diffusion constants of a number of polycyclic aromatic hydrocarbons (Table 1) shows an inverse dependence on van der Waals radius (Fig. 1). The relation, however, compares poorly with the Stokes–Einstein relation [eqn. (1)] unless a correction is used for the radius. Fig. 2 shows the correspondence between the van

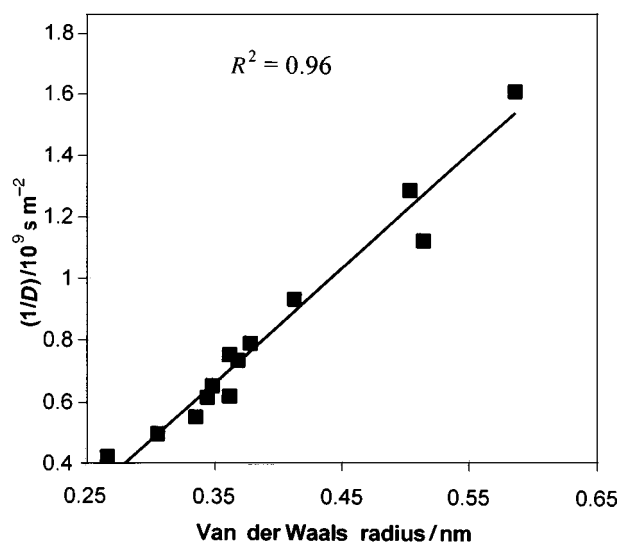


Fig. 1 Dependence of $1/\text{self-diffusion constant}$ as measured by NMR on the calculated van der Waals radius

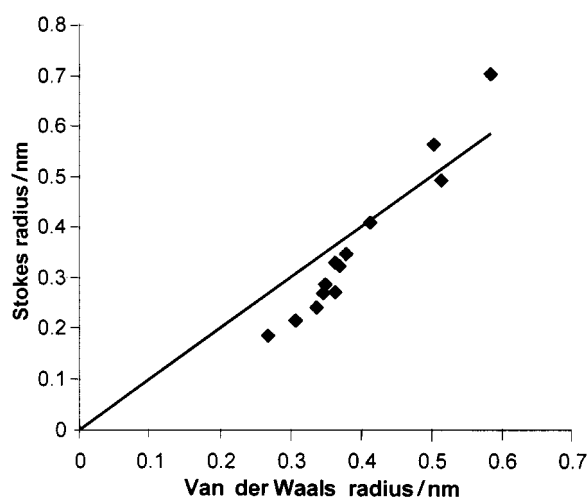


Fig. 2 Relationship between Stokes radius and van der Waals radius for neutral polycyclic aromatic hydrocarbons in $[^2\text{H}_8]\text{THF}$

der Waals and Stokes radius [eqn. (2)] given that the viscosity (η) of $[^2\text{H}_8]\text{THF}$ is $5.01 \times 10^{-4} \text{ kg m}^{-1} \text{ s}^{-1}$ (5.01 millipoise).¹³

Effects of salt formation on self-diffusion

Salt formation decreases the self-diffusion constant indicating a significant increase in moiety size. The reduction in self-diffusion constant (between 20 and 51%) varies from anion to anion.¹⁴ However, in general the greater the ionization, the more the self-diffusion is slowed. An extreme example is the self-diffusion constant of Li^+ in dilute aqueous LiCl that is $9.6 \times 10^{-10} \text{ m}^2 \text{ s}^{-1}$.¹⁵ Using the Stokes–Einstein relation the self-diffusion constant of Li^+ would be expected to be $5.7 \times 10^{-9} \text{ m}^2 \text{ s}^{-1}$, nearly six times higher than observed. Polycyclic aromatic hydrocarbon salts in ethereal solution are much less solvated. Nevertheless, the increase in moiety size indicated by the Stokes–Einstein relation is far too great to be accounted for by the addition of the cation (0.4 to 5%). In most cases it is too great to be accounted for by dimerization (21%) even where other evidence does not suggest aggregation.

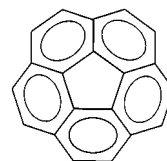
The increase in apparent size may therefore come from the solvent shell that accompanies polarized species. Table 2 shows the diffusion parameters. However, estimates of the numbers of solvent molecules in the solvent shell are only approximate as they depend on the sixth root of the calibration of the gradient strength. There is evidence that the number of solvent molecules increases with the ionization of the molecule. However,

Table 2 Self-diffusion constants of lithium salts of polycyclic aromatic hydrocarbons, Stokes radii in $[^2\text{H}_8]\text{THF}$ at 298 K

Compound	Charge	$D/10^{-9} \text{ m}^2 \text{ s}^{-1a}$	Stokes Radius/nm
9-Hydroanthracene monoanion	-1	1.00	0.44
Anthracene	-2	0.90	0.48
Corannulene	-4	0.65	0.67
9,10-Dimethyl-9-hydroanthracene monoanion	-1	0.91	0.48
9,10-Dimethylantracene	-2	0.91	0.49
9,10-Diphenyl-9-hydroanthracene monoanion	-1	0.77	0.56
9,10-Diphenylantracene	-2	0.74	0.58
1,8-Dicorannulenyl octane	-8	0.50	0.87
Penta- <i>tert</i> -butylcorannulene	-2	0.71	0.62
Penta- <i>tert</i> -butylcorannulene	-4	0.62	0.70

^a $\pm 2\%$.

slight experimental and theoretical errors lead to large changes in the number of solvent molecules calculated. Therefore, more accurate observations are required in order to reach firm conclusions. The solvent shell is in a state of constant flux so the number of molecules involved is dependent on the timescale used to measure it.⁶ The smaller the timescale, the larger the solvent shell. On the NMR timescale (milliseconds to seconds) no signals arise from the bound solvent molecules. On the UV–VIS timescale (femtoseconds), solvation effects can be resolved.⁶ The diffusion timescale is several collisions of the order of 100 ps. On timescales shorter than the time between collisions the concept of a solvent shell becomes meaningless anyway because, without molecular collisions, there is no test as to whether the molecule is bound. It is therefore the diffusion timescale that is of greatest physical and chemical importance.



Corannulene

In the case of corannulene, it is known that the tetraanion with lithium is dimeric from other studies.^{16,17} A mixture of anions of corannulene and *tert*-butylcorannulene yields signals arising from mixed dimers.^{16,17} We attempted to find evidence for dimerization for other anions (anthracene, tetracene and 9,10-dimethylantracene) but failed. No mixed dimers appeared in the spectrum even at low temperatures and the chemical shifts and self-diffusion constants were found to be almost independent of concentration up to 10 mmol dm^{-3} . The lack of mixed dimers is strong evidence against dimerization. However, the lack of a concentration effect does not rule out aggregation. It merely rules out weak aggregation. The corannulene tetraanion with lithium does not show significant chemical shift changes with concentration down to the detection limit of ^1H NMR spectroscopy. This is still consistent with a strongly bound dimer that does not undergo further aggregation.

The self-diffusion constant varies with anion (Table 2) more than for cation (Table 3). The cation is small relative to the anion and therefore has little effect in itself. The solvation shell does have a large effect but its outer reaches are similar whether the cation is lithium or caesium. As a result the self-diffusion constants of salts with different metals are similar.

The outer parts of the solvent shell affect self-diffusion measurements. Therefore, they are barely affected by the inner solvation state of the ion pair (triplet, quintet, etc.). Hence, self-diffusion constants are not able to differentiate between solvent

Table 3 Self-diffusion constants of dimetallic salts of 9-phenylanthracene in $[^2\text{H}_8]\text{THF}$

Metal	$D/10^{-9} \text{ m}^2 \text{ s}^{-1}$ ^a
Li	0.94
Na	0.81
K	0.85
Rb	0.88
Cs	1.06

^a $\pm 2\%$.**Table 4** Parameters for Eyring model for self-diffusion constants of various solvents

Solvent	$\eta_0/10^{-8} \text{ kg m}^{-1} \text{ s}^{-1}$	$W/10^3 \text{ mol J}^{-1}$	r_s/nm
NH_3	2.1	7.8	0.15 ^a
MeOMe	4.4	6.4	0.12 ^b
THF	5.3	8.4	0.15 ^c
$[^2\text{H}_8]\text{THF}$	4.2	9.2	0.17 ^d
DME	1.6	10.7	0.18 ^b

^a Assuming $\eta = 2.55 \times 10^{-4} \text{ kg m}^{-1} \text{ s}^{-1}$ at 239.65 K.²⁰ ^b Estimated Stokes radius. ^c Assuming $\eta = 4.64 \times 10^{-4} \text{ kg m}^{-1} \text{ s}^{-1}$ at 298 K.¹³ ^d Assuming $\eta = 5.01 \times 10^{-4} \text{ kg m}^{-1} \text{ s}^{-1}$.

separated or contact ions. Such solvation states can be studied by chemical shift or UV absorption frequency dependence on temperature.^{1-6,18} However, if the ions were freely separated then the self-diffusion constant of the cations would be much greater than for the anions. We measured the self-diffusion constant of Li to be the same as its anion for anthracene in $[^2\text{H}_8]\text{THF}$ and NH_3 . This is clear evidence that the ions are tightly bound on the diffusion timescale. The other alkali metals have a higher quadrupolar moment and resonate at lower frequencies than lithium, hence their relaxation rates are much faster and their low gyromagnetic ratio make self-diffusion measurements more difficult. As a result we were unable to measure their self-diffusion rates although equipment exists that can do so with the possible exception of potassium. The self-diffusion rate of potassium in these salts is probably unmeasurable with current technology because of its very low gyromagnetic ratio.

Temperature dependence of self-diffusion constant

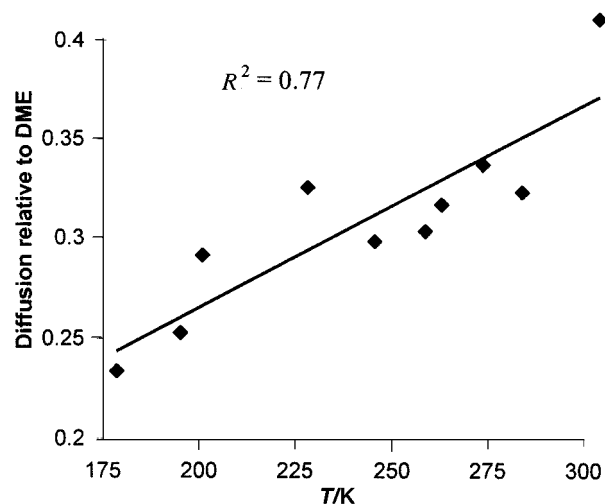
Self-diffusion constants are very temperature dependent. In the Stokes-Einstein relation [eqn. (1)], not only is there a temperature term but the viscosity (η) is temperature dependent [eqn. (3), where η_0 is a constant and W is the 'rate constant of

$$\eta = \eta_0 T e^{\frac{W}{RT}} \quad (3)$$

viscosity' and R is the gas constant ($8.3143 \text{ J mol}^{-1} \text{ K}^{-1}$).^{18,19} Over a range of 100 K the self-diffusion constant of THF increases by a factor of 5.4 ($4.9 \times 10^{-10} \text{ m}^2 \text{ s}^{-1}$ at 200 K and $2.64 \times 10^{-9} \text{ m}^2 \text{ s}^{-1}$ at 300 K). This is the reason that we were very careful to calibrate the temperature for each measurement. The self-diffusion constant of THF behaves approximately in accordance with eqn. (4), where r_s [Stokes radius calculated

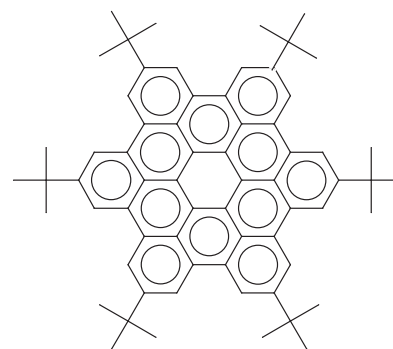
$$D = \frac{k_B}{6\pi r_s \eta_0} e^{\frac{W}{RT}} \quad (4)$$

from eqn. (2)] = 0.150 nm, $\eta_0 = 5.3 \times 10^{-8} \text{ kg m s}^{-1}$ and $W = 8440 \text{ mol J}^{-1}$. Table 4 lists the values for other solvents. The 'rate constants' (W) increase with the molecular weight for the ethers while that of ammonia is slightly larger than expected, probably because of hydrogen bonding. These values were not perfect and deviations of up to 5% are observed over the tem-

**Fig. 3** Dependence upon temperature of relative self-diffusion constant of disodium 9,10-dihydroanthracenediide in DME

perature range. While 5% is small compared with the change of 81% in the absolute self-diffusion constant the simple Eyring model^{19,21} was not sufficient for our purposes.

The accuracy of the Eyring model [eqn. (3)] is not sufficient to detect small changes in moiety radius with temperature. However, the temperature dependence of self-diffusion constant should be the same for all particles in solution provided that the particle size is independent of temperature. For neutral PAHs we found that this was the case. To demonstrate this, we used a solution of anthracene and hexakis(*tert*-butyl-

Hexakis(*tert*-butylbenzo)coronene

benzo)coronene in THF. Therefore, this method of comparison can be used for determining changes in moiety radius with temperature. The self-diffusion constant relative to that of the solvent varies much more with temperature for charged species than for neutral molecules. The relative self-diffusion constant increases with temperature. We observed the effect in ammonia, dimethyl ether, THF and dimethoxyethane. The effect was strongest in THF and weakest in ammonia that is consistent with a solvation effect. Fig. 3 shows the relative self-diffusion constant's temperature dependence for disodium 9,10-dihydroanthracenediide in DME. The change in relative self-diffusion constant was $1.3 \times 10^{-3} \text{ K}^{-1}$ in $[^2\text{H}_8]\text{THF}$, $1.0 \times 10^{-3} \text{ K}^{-1}$ in DME and $5 \times 10^{-4} \text{ K}^{-1}$ in MeOMe. The effect was negligible within experimental error (10^{-4} K^{-1}) for lithium 9,10-dihydroanthracenediide in NH_3 . A different salt was studied in NH_3 because the dianion is not formed. A significant temperature dependence of relative self-diffusion rate was observed for lithium 9,10-dihydroanthracenediide, dilithium 9,10-dihydroanthracenediide and disodium 9,10-dihydroanthracenediide in $[^2\text{H}_8]\text{THF}$. The changes in self-diffusion constant for THF and DME are equivalent to adding about one solvent molecule per 50 K of cooling.

Experimental

^1H and ^7Li NMR spectra were recorded on a Bruker DRX-400 spectrometer with a BGU II gradient amplifier unit and a 5 mm BBI probe equipped with a z -gradient coil. As alkali metals react with TMS, chemical shifts were measured relative to the most downfield solvent peak that had in turn been calibrated against TMS. In the temperature range 209 to 304 K, the chemical shift of NH_3 was $0.732 - (2.83 \times 10^{-3} T')$. In the temperature range 186 to 304 K, the chemical shift of MeOMe is $3.2133 + (4.2 \times 10^{-5} T')$. In the temperature range 155 to 390 K the chemical shift of H1 of $[^2\text{H}_7]\text{THF}$ in $[^2\text{H}_8]\text{THF}$ is $3.5749 + (4.71 \times 10^{-5} T') - (5.1 \times 10^{-8} T'^2) + (8.2 \times 10^{-10} T'^3) - (3.3 \times 10^{-12} T'^4)$ ppm.⁷ The regular THF H1 is 0.0369 ppm upfield of the signal for the deuterated solvent. In the temperature range 242 to 300 K, the chemical shift of the CH_2 of diethyl ether is $3.3769 + (2.40 \times 10^{-4} T')$. In the temperature range 200 to 300 K, the chemical shift of the DME methyl signal is $3.4280 + (1.92 \times 10^{-4} T')$, where $T' = \text{temperature} - 295 \text{ K}$. The temperature was determined using a standard methanol NMR thermometer.^{22,23}

Materials

Commercial samples of anthracene, 9-methylanthracene, 9,10-dimethylanthracene, naphthalene, pyrene, tetracene, 9-phenylanthracene and 9,10-diphenylanthracene were purified by recrystallization. Corannulene was synthesized using the method of Scott *et al.*²⁴ The NMR spectra of 9-methylanthracene,²⁵ 9,10-dimethylanthracene,²⁵ 9-phenylanthracene,²⁵ corannulene,²⁶ dilithium 9-phenyl-9,10-dihydroanthracenediide,⁷ disodium 9-phenyl-9,10-dihydroanthracenediide,³¹ dipotassium 9-phenyl-9,10-dihydroanthracenediide,⁷ dirubidium 9-phenyl-9,10-dihydroanthracenediide,⁷ dicaesium 9-phenyl-9,10-dihydroanthracenediide,⁷ dilithium 9,10-diphenyl-9,10-dihydroanthracenediide⁷ and tetralithium corannulenetetraide²⁶ are reported elsewhere.

Solvents

NH_3 , MeOMe, THF and $[^2\text{H}_8]\text{THF}$ were dried and degassed as previously reported.⁶ The solvent was placed in a flask and connected to a vacuum line then degassed with several freeze-pump-thaw cycles before being vacuum transferred into a flask containing distilled Na:K, 5:1 alloy. This was then sonicated (unnecessary for NH_3) until dry for several minutes. NH_3 goes very dark blue, and THF (and $[^2\text{H}_8]\text{THF}$) turns light blue. No color change is observed for MeOMe. DME was prepared by the same method but using LiAlH_4 instead of the alloy.

Preparation of anions

The alkali metal was placed into the upper part of the tube containing the polycyclic aromatic hydrocarbon (~1 mg to yield ~2 mM solutions). Lithium was inserted into the tube under argon while the other alkali metals were distilled into the tube. Dry $[^2\text{H}_8]\text{THF}$ was vacuum transferred into the tube, which was then sealed under vacuum.²⁷ Repeated inversion of the tube brought the solution into contact with the metal. ^1H NMR spectroscopy was used to detect the formation of the anions.

Self-diffusion measurement by NMR spectroscopy

We used the pulsed field gradient stimulated spin-echo (PFG-SSE)²⁸⁻³¹ (Fig. 4) because it is most suitable for systems where T_1 is long relative to T_2 or where there is homonuclear spin-spin coupling the latter being the case for the systems studied. The advantage of the stimulated spin-echo is that its intensity is largely dependent on longitudinal relaxation time [T_1 , eqn. (5), where I is the observed intensity, I_0 is the intensity

$$I = \frac{I_0}{2} e^{-\frac{\tau_1}{T_1} - \frac{2\tau_2}{T_2} - (\gamma G \delta)^2 D (\Delta - \frac{\delta}{3})} \quad (5)$$

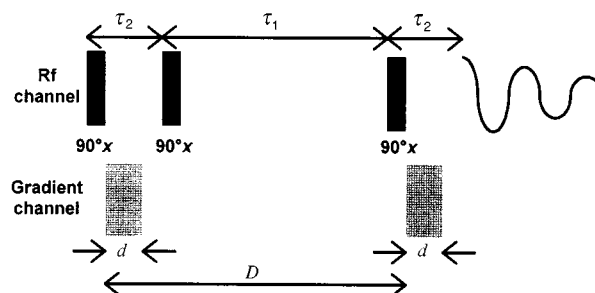


Fig. 4 Pulse sequence for measuring self-diffusion constants. Pulsed field gradient stimulated spin-echo sequence.

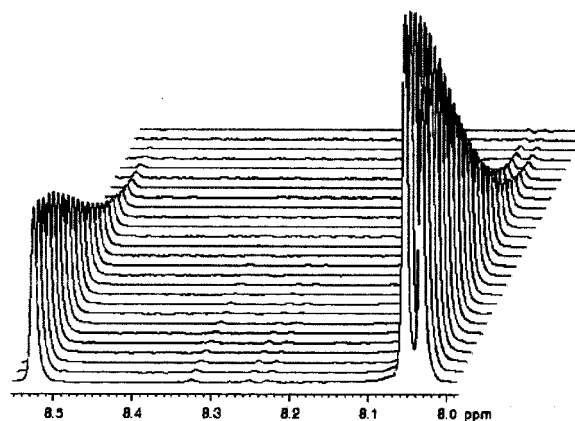


Fig. 5 Part of the self-diffusion spectrum of 9-phenylanthracene in $[^2\text{H}_8]\text{THF}$ at 298 K

for a single pulse experiment, τ_1 is the time between the second and third pulses, τ_2 is the time between the first two pulses, γ is the gyromagnetic ratio, G is the gradient strength, D is the self-diffusion constant, δ is the gradient pulse length and Δ is the time between the start of the first gradient pulse and the start of the second]. Good results were obtained for coupled systems provided that the time that the magnetization was in the xy plane prior to acquisition was restricted to 8 ms. We used a gradient pulse length of 3.5 ms and adjusted Δ in order to yield a good dynamic range for gradient strengths up to 50 G cm^{-1} . If the self-diffusion constant was too slow to be measured accurately with such a short gradient pulse length then the pulse length was increased.

The gradient was calibrated using a cylindrical glass phantom sandwiched between two glass tubes and a hollow glass cylinder sandwiched between glass rods and recording the ^1H or ^2H NMR spectrum of the phantom immersed in solvent with the gradient on. The spectrum contained a broad signal with a rectangular depression which corresponds to the phantom. The width of the depression (solid cylinder) or central peak (hollow cylinder) is proportional to the gradient strength [eqn. (6), where $\Delta\omega$ is the width of the depression and

$$\Delta\omega = \gamma G l \quad (6)$$

l is the length of the phantom]. No significant deviation from linearity with gradient strength was detectable as is to be expected from other reports.³² The maximum gradient strength on the spectrometer was 0.537 T m^{-1} in non-polar solvents regardless of temperature. The calibration was repeated many times and the estimated error is 0.8% leading to an absolute error in the self-diffusion constant of 1.6%. Self-diffusion constants measured for THF with this calibration agreed with literature values¹³ to within the experimental error. The diffusion experiment yields spectra of the type shown in Fig. 5 where

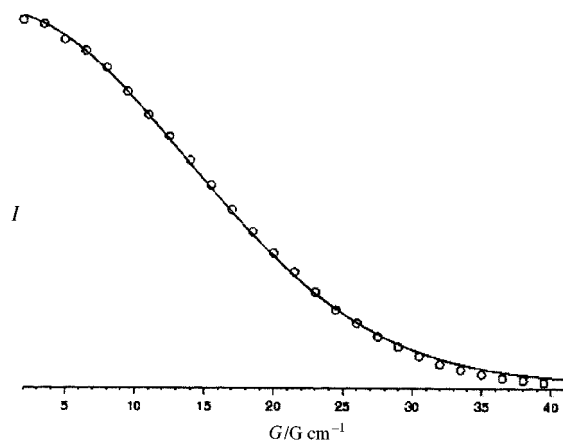


Fig. 6 Plot of intensity against gradient strength fitted to a Gaussian curve for the left signal in Fig. 5

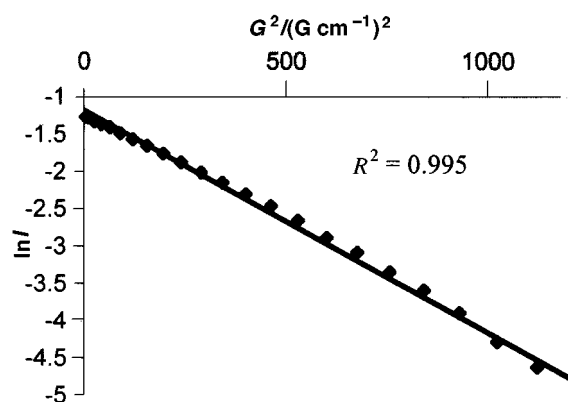


Fig. 7 Plot of the natural log intensity against the square of the gradient strength for the left signal in Fig. 5

the signal decays in a Gaussian manner with increasing gradient strength. A plot of the signal intensity against gradient strength fits the theoretical Gaussian curve well (Fig. 6). A plot of natural log intensity against the square of the gradient strength yields an excellent fit (Fig. 7). However, such a fit does not take into account the greater relative error due to noise for the less intense signals. We obtained more accurate values for self-diffusion constants by using a non-linear fit of the Gaussian curve to the actual intensities (Fig. 6).

Anthracene

$\delta_{\text{H}}([^2\text{H}_8]\text{THF}; 298 \text{ K})$ 7.42 and 8.00 (AA'XX', each 4 H) and 8.44 (s, 2 H); $^{25}\delta_{\text{H}}(\text{THF}; 298 \text{ K})$ same as for $[^2\text{H}_8]\text{THF}$ to within 0.01 ppm; $\delta_{\text{H}}(\text{NH}_3; 298 \text{ K})$ 7.57 and 8.15 (AA'XX', each 4 H) and 8.60 (s, 2 H); $\delta_{\text{H}}(\text{MeOMe}; 298 \text{ K})$ 7.41 and 7.98 (AA'XX', each 4 H) and 8.42 (s, 2 H).

Corannulene

Corannulene was synthesized using the method of Scott *et al.*²⁴ $\delta_{\text{H}}([^2\text{H}_8]\text{THF and THF}; 298 \text{ K})$ 7.93 (s, 10 H).

1,8-Dicorannulenyl-octane

1,8-Dicorannulenyl-octane was synthesized using the method of Cheng.³³ $\delta_{\text{H}}([^2\text{H}_8]\text{THF and THF}; 298 \text{ K})$ 1.49 (tt, 4 H), 1.59 (tt, 4 H), 1.94 (tt, 4 H), 3.17 (t, 4 H), 7.61 (s, 2 H), 7.74 (d, 2 H), 7.78 (d, 2 H), 7.80 (AB, total 4 H), 7.81 (AB, total 4 H), 7.84 (d, 2 H), 7.98 (d, 2 H).

Penta-*tert*-butylcorannulene

Penta-*tert*-butylcorannulene was synthesized using the method of Cheng.³³ $\delta_{\text{H}}([^2\text{H}_8]\text{THF and THF}; 298 \text{ K})$ 1.72 (s, 45 H), 8.17 (s, 5 H).

Hexakis(*tert*-butylbenzo)coronene

Hexakis(*tert*-butylbenzo)coronene was synthesized using the method of Müllen *et al.*^{34,35} $\delta_{\text{H}}([^2\text{H}_8]\text{THF and THF}; 298 \text{ K})$ 1.83 (s, 54 H) and 9.42 (s, 12 H).

Lithium 9,10-dihydroanthracene

$\delta_{\text{H}}([^2\text{H}_8]\text{THF}; 298 \text{ K})$ 3.50 (s, 2 H), 4.00 (s, 1 H), 6.00 (t, 2 H), 6.24 (d, 2 H), 6.48 (t, 2 H), 6.54 (d, 2 H); $\delta_{\text{H}}(\text{NH}_3; 298 \text{ K})$ 3.58 (s, 2 H), 4.58 (s, 1 H), 5.77 (t, 2 H), 6.00 (d, 2 H), 6.38 (t, 2 H), 6.39 (d, 2 H); $\delta_{\text{H}}(\text{MeOMe}; 298 \text{ K})$ 3.92 (s, 2 H), 5.02 (s, 1 H), 6.11 (t, 2 H), 6.37 (d, 2 H), 6.57 (t, 2 H), 6.64 (d, 2 H).

Dilithium 9,10-dihydroanthracenediide

$\delta_{\text{H}}([^2\text{H}_8]\text{THF}; 298 \text{ K})$ 1.88 (s, 2 H), 3.36 and 4.25 (AA'XX', each 4 H); $^7\delta_{\text{H}}(\text{MeOMe}; 298 \text{ K})$ 2.17 (br, 2 H), 3.66 (br, 4 H) and 4.48 (br, 4 H).

Disodium 9,10-dihydroanthracenediide

$\delta_{\text{H}}([^2\text{H}_8]\text{THF}; 298 \text{ K})$ 1.48 (s, 2 H), 2.80 and 3.78 (AA'XX', each 4 H); $^{25}\delta_{\text{H}}(\text{MeOMe}; 298 \text{ K})$ 1.79 (br, 2 H), 3.10 (br, 4 H) and 4.00 (br, 4 H); $\delta_{\text{H}}(\text{DME}; 298 \text{ K})$ 1.53 (br, 2 H), 2.85 (br, 4 H) and 3.83 (br, 4 H).

Lithium 9,10-dimethyl-9,10-dihydroanthracene

$\delta_{\text{H}}([^2\text{H}_8]\text{THF}; 298 \text{ K})$ 0.91 (d, 3 H), 1.73 (s, 3 H), 3.49 (q, 1 H), 5.72 (t, 2 H), 6.07 (d, 2 H), 6.39 (d, 2 H) and 6.46 (t, 2 H).

Dilithium 9,10-dimethyl-9,10-dihydroanthracenediide

$\delta_{\text{H}}([^2\text{H}_8]\text{THF}; 298 \text{ K})$ 0.58 (s, 6 H) and 3.86 and 4.81 (AA'XX', each 4 H).

Lithium 9,10-diphenyl-9,10-dihydroanthracene

$\delta_{\text{H}}([^2\text{H}_8]\text{THF}; 298 \text{ K})$ 4.82 (s, 1 H), 5.85 (t, 2 H), 6.31 (t, 2 H), 6.56 (d, 2 H), 6.61 (d, 2 H), 6.73 (t, 2 H), 6.84 (t, 1 H), 6.90 (t, 1 H), 6.94 (t, 2 H), 7.08 (d, 2 H), 7.10 (d, 2 H).

Dilithium 9,12-dihydrotetracenediide

$\delta_{\text{H}}([^2\text{H}_8]\text{THF}; 175 \text{ K})$ 2.79 (s, 4 H) and 4.28 and 4.71 (AA'XX', each 4 H).

Dilithium penta-*tert*-butylcorannulenediide

$\delta_{\text{H}}([^2\text{H}_8]\text{THF and THF}; 298 \text{ K})$ -3.37 (s, 5 H), -1.56 (s, 45 H).

Octalithium 1,8-dicorannulenyl-octane

$\delta_{\text{H}}([^2\text{H}_8]\text{THF and THF}; 298 \text{ K})$ 2.2–3.2 (m, 16 H), 6.7–7.2 (m, 18 H).

Conclusions

Self-diffusion is a useful tool for comparing sizes of molecules. NMR and specifically the PFG-SSE method is a good way of measuring self-diffusion constants with an accuracy of $\pm 1\%$ achievable. For a set of similar molecules, it is possible to obtain a reasonably predictable ($\pm 10\%$) correlation with molecular size. Solvation shells complicate the measurement of charged systems. However, the self-diffusion constant can be used to study these solvation shells: comparing solvents and estimating their size. The size of the solvation shell varies widely with anion but not with cation. The solvation effect is strongest for $\text{THF} \approx \text{DME} > \text{MeOMe} > \text{NH}_3$. Self-diffusion measurements provide unequivocal proof that the lithium salts are not free ions in solution.

Acknowledgements

We thank the German-Israel Foundation for Scientific Research and Development (G. I. F.) and the US Department of Energy for financial support. We thank Dr Serge Boentges (Bruker Spectrospin) for helping us set up the self-diffusion experiments and Dr Yoram Cohen for fruitful discussions.

References

- 1 D. Nicholls and M. Szwarc, *J. Am. Chem. Soc.*, 1966, **88**, 5757.
- 2 D. Nicholls and M. Szwarc, *Proc. R. Soc. A, London*, 1967, **301**, 223.
- 3 D. Nicholls and M. Szwarc, *Proc. R. Soc. A, London*, 1967, **301**, 231.
- 4 A. Sygula and P. W. Rabideau, *J. Org. Chem.*, 1987, **52**, 3521.
- 5 P. W. Rabideau, *Tetrahedron*, 1989, **45**, 1579.
- 6 R. E. Hoffman, M. Nir, I. O. Shapiro and M. Rabinovitz, *J. Chem. Soc., Perkin Trans. 2*, 1996, 1225.
- 7 M. Nir, I. O. Shapiro, R. E. Hoffman and M. Rabinovitz, *J. Chem. Soc., Perkin Trans. 2*, 1996, 1607.
- 8 W. E. Rhine, J. Davis and G. D. Stucky, *J. Am. Chem. Soc.*, 1975, **97**, 2079.
- 9 L. G. Longworth, *J. Am. Chem. Soc.*, 1952, **74**, 4155.
- 10 L. G. Longworth, *J. Phys. Chem.*, 1960, **64**, 1914.
- 11 H. J. Tyrrell and K. R. Harris, *Diffusion in Liquids*, Butterworths, London, 1984.
- 12 J. P. Hansen and I. R. McDonald, *Theory of Simple Liquids*, Academic Press, London, 1960.
- 13 M. Holz, X.-A. Mao, D. Seiferling and A. Sacco, *J. Chem. Phys.*, 1996, **104**, 669.
- 14 Y. Cohen and A. Ayalon, *Angew. Chem., Int. Ed. Engl.*, 1995, **34**, 816.
- 15 M. Holz and H. Weingärtner, *J. Magn. Reson.*, 1991, **92**, 115.
- 16 A. Ayalon, A. Sygula, P.-C. Cheng, M. Rabinovitz, P. W. Rabideau and L. T. Scott, *Science*, 1994, **265**, 1065.
- 17 A. Ayalon, PhD Thesis, Hebrew University of Jerusalem, 1993.
- 18 M. Daney, H. Bouas-Laurent, B. Calas, L. Giral and N. Platzer, *J. Organomet. Chem.*, 1980, **188**, 277.
- 19 S. Glasstone, K. J. Laidler and H. Eyring, *Theory of Rate Processes*, McGraw-Hill, New York, 1941.
- 20 R. C. Weast and M. J. Astle, *CRC Handbook of Chemistry and Physics*, CRC Press, Boca Raton, FL, 1981.
- 21 P. A. Egelstaff, *An Introduction to the Liquid State*, Academic Press, London, 1967.
- 22 A. L. Van Geet, *Anal. Chem.*, 1968, **40**, 2227.
- 23 A. L. Van Geet, *Anal. Chem.*, 1970, **42**, 679.
- 24 L. T. Scott, M. M. Hashemi, D. T. Meyer and H. B. Warren, *J. Am. Chem. Soc.*, 1991, **113**, 7082.
- 25 M. Nir, R. E. Hoffman, I. O. Shapiro and M. Rabinovitz, *J. Chem. Soc., Perkin Trans. 2*, 1995, 1433.
- 26 A. Ayalon, M. Rabinovitz, P.-C. Cheng and L. T. Scott, *Angew. Chem., Int. Ed. Engl.*, 1992, **31**, 1636.
- 27 I. O. Shapiro, M. Nir, R. E. Hoffman and M. Rabinovitz, *J. Chem. Soc., Perkin Trans. 2*, 1994, 1519.
- 28 J. E. Tanner, *J. Chem. Phys.*, 1970, **52**, 2523.
- 29 P. Stilbs, *Prog. Nucl. Magn. Reson. Spectrosc.*, 1987, **19**, 1.
- 30 R. M. Cotts, M. J. R. Hoch, T. Sun and J. T. Markert, *J. Magn. Reson.*, 1989, **83**, 252.
- 31 S. S. Pochapsky, H. Mo and T. C. Pochapsky, *J. Chem. Soc., Chem. Commun.*, 1995, 2513.
- 32 C. Herdlicka, J. Rischter and M. D. Zeidler, *Z. Naturforsch., Teil A*, 1988, **43**, 1075.
- 33 P.-C. Cheng, Dissertation, Boston College, 1996.
- 34 A. Stabel, P. Herwig, K. Müllen and J. P. Rabe, *Angew. Chem., Int. Ed. Engl.*, 1995, **34**, 1609.
- 35 P. Herwig, C. W. Kayser, K. Müllen and H. W. Spiess, *Adv. Mater.*, 1996, **8**, 510.

Paper 8/00382C
Received 14th January 1998
Accepted 15th April 1998